Geochemistry, Geophysics, Geosystems

RESEARCH ARTICLE
10.1029/2018GC008005

Key Points:
- Provenance studies can greatly benefit from the U-Pb dating of multiple detrital minerals
- Combining trace element measurement with dating can help fingerprint source rock types for detrital zircon, monazite, rutile, and titanite
- An example of the multiproxy approach utilizing four different minerals is provided here in a study of New England river sand

Supporting Information:
- Supporting Information S1
- Table S1

Correspondence to:
R. M. Gaschnig,
richard_gaschnig@uml.edu

Citation:
Gaschnig, R. M. (2019). Benefits of a multiproxy approach to detrital mineral provenance analysis: An example from the Merrimack River, New England, USA. *Geochemistry, Geophysics, Geosystems*, *19*. https://doi.org/10.1029/2018GC008005

Received 5 OCT 2018
Accepted 2 MAR 2019
Accepted article online 5 MAR 2019

Benefits of a Multiproxy Approach to Detrital Mineral Provenance Analysis: An Example from the Merrimack River, New England, USA

Richard M. Gaschnig[1]

[1]Department of Environmental, Earth and Atmospheric Sciences, University of Massachusetts Lowell, Lowell, MA, USA

Abstract The advantages in provenance research of U-Pb dating different detrital minerals along with simultaneously analyzing trace elements is demonstrated in a study of sand from the mouth of the Merrimack River in New England, USA. Zircon ages record episodes of magmatism in the Early Paleozoic, peaking in the Early Devonian, followed by quiescence through the remainder of the Paleozoic and additional magmatic episodes in the Jurassic and Cretaceous. Simultaneous measurement of trace elements in zircons reveals a shift from arc magmatism to crustal melting associated with terrane collision in the Early Devonian, while many Jurassic grains are clearly derived from A-type granites. Detrital monazites and rutiles have Devonian and Permian ages. Many of the older monazites have trace element characteristics suggestive of igneous origin, while Permian monazites are clearly metamorphic and record orogenesis that is absent from the detrital zircon record. Rutile grains have trace element chemistry indicative of mostly metasedimentary source rocks, and Zr thermometry indicates growth under amphibolite facies conditions. Age offsets between monazite and rutile populations provide information about the region's cooling history. Titanite grains have trace element chemistry mostly consistent with igneous origin and U-Pb ages lining up with minor zircon age populations in the Ordovician-Silurian and the Middle Devonian, suggesting that these magmatic episodes produced metaluminous compositions. These results show that combining trace element fingerprinting with dating and analyzing multiple detrital mineral species provide a more complete portrait of the geologic history of the sediment source region than U-Pb dating of zircon alone.

1. Introduction

The dating of detrital zircons in sands and sandstones is a premier tool in studies of sedimentary provenance, paleogeography, orogenic cycling, and crustal growth. Gehrels (2015) noted an exponential increase in the publication and use of detrital zircon age data in the first decade of this century, coinciding with the advent of zircon dating by laser ablation-inductively coupled plasma-mass spectrometry (LA-ICP-MS); by 2010, roughly 2,000 publications a year were presenting or discussing detrital zircon data (Gehrels, 2015).

Detrital zircon dating provides an essential foundation of information in provenance studies, but it does not always provide a complete record of the geologic history of sediment source regions, a fact that has long been recognized. As a primarily igneous mineral formed chiefly in intermediate and felsic magmas, the detrital zircon record will underrepresent any mafic magmatism that a region has experienced and provide limited information on the metamorphic history of a region. For example, numerous studies in the Appalachians have noted that both Paleozoic clastic sequences and modern rivers are dominated by ~1-Ga Grenvillian detrital zircon and have only limited numbers of grains corresponding to the Paleozoic Appalachian orogenies, with the climactic Alleghanian orogeny sometimes completely absent from the detrital zircon record (Eriksson et al., 2003, 2004; Gray & Zeitler, 1997; Thomas et al., 2004). Moecher and Samson (2006) attributed this to the zircon richness or high "zircon fertility" of Grenvillian basement, the extreme durability of zircon leading to its survival through multiple sedimentary cycles, and the limited growth of new zircon during Paleozoic metamorphism of the Appalachian sedimentary sequences. Furthermore, as is bound to sometimes occur when a single tool is considered, detrital zircon age spectra sometimes produce nonunique provenance signatures (Slagstad & Kirkland, 2017). For example, LaMaskin (2012) noted that Cordilleran basins that formed thousands of kilometers apart often have identical detrital zircon age spectra.

Numerous additional tools for detrital mineral provenance research have been proposed and shown to be effective in complementing detrital zircon age spectra and compensating for the limits of detrital zircon

dating. These include (and are certainly not limited to) LA-ICP-MS or SHRIMP U-Pb dating of other minerals such as monazite and rutile (Hietpas et al., 2010; O'Sullivan et al., 2016; Zack et al., 2011), common Pb isotope analysis of detrital feldspar (Clift et al., 2001; Tyrrell et al., 2006), and analysis of trace elements and isotopic tracers in zircon (Barth et al., 2013; Iizuka et al., 2013; Morag et al., 2011; Stewart et al., 2010) and other minerals such as rutile (Zack, von Eynatten, & Kronz, 2004), along with thermochronological methods, such as fission track and U-Th-He dating of detrital zircon and apatite (e.g., Naeser et al., 2016; Painter et al., 2014; Reiners, 2005) and Ar-Ar dating of detrital muscovite (e.g., Copeland et al., 2015; Hodges et al., 2005) Usage and combination of these other techniques remain the exception rather than the rule in provenance research, with zircon dating (and more recently, zircon Hf isotope analysis) remaining the standard tool of the trade.

The purpose of this contribution is to provide new emphasis on the benefits of a multiproxy approach in sand and sandstone provenance research. I demonstrate the utility of examining the U-Pb age populations of monazite, rutile, and titanite, in addition to zircon, from a modern sedimentary system, along with simultaneous trace element characterization, all accomplished on a single instrument package (i.e., a laser and quadrupole inductively coupled plasma-mass spectrometer). Built upon the foundation of detrital zircon age data, these additional layers of information provide an expanded portrait of the igneous, metamorphic, and cooling history of New England, along with the potential tectonic settings of the sediment source rocks.

2. Background

2.1. The Sample and Geologic Setting

The target of this study is a sample (latitude-longitude of 42.789°, −70.807°) of garnet-rich sand from Plum Island in northeastern Massachusetts. Plum Island is a barrier island that extends south from the mouth of the Merrimack River and is composed largely of sediment derived from that river. The Merrimack River (Figure 1) drains most of the southern half of New Hampshire and a portion of northeastern Massachusetts and traverses several of the major tectonomagnatic elements of the Northern Appalachians. The oldest rocks in the Merrimack River drainage basin are the Neoproterozoic Massabesic gneiss, Neoproterozoic arc rocks of the Avalon terrane, and Neoproterozoic through Ordovician arc rocks of the Nashoba terrane (Acaster & Bickford, 1999; Dorais et al., 2012; Thompson et al., 2012). Silurian and Devonian metasedimentary rocks are exposed extensively throughout the drainage basin, along with belts of plutons from the Acadian (Early Devonian), Neoacadian (Late Devonian to Mississippian), and Alleghanian (Pennsylvanian to Permian) orogenies (e.g., Bradley & Tucker, 2002; Dorais, 2003; Lyons et al., 1997; Robinson et al., 1998; Tomascak et al., 1996). Voluminous A-type granitic magmatism also occurred in the Mesozoic, producing the older (Late Triassic and Jurassic) and younger (Cretaceous) White Mountains igneous provinces (e.g., Eby et al., 1992).

3. Methods

3.1. Mineral Separation

A sample of garnet-rich Plum Island sand was initially panned to concentrate the heavy mineral fraction. A Frantz magnetic separator was used (0.3 A at 25° side tilt setting) to remove the most magnetically susceptible minerals, including most of the garnet, before the remaining sand was run through methylene iodide to further concentrate the heavy minerals. These were returned to the Frantz to separate monazite, titanite, rutile, and zircon. Monazite was found to be concentrated in the magnetic fraction between 0.5 and 0.6 A (25° side tilt). Titanite was recovered from the magnetic fraction between 0.8 and 1.5 A (25° side tilt), while rutile and zircon were isolated together in the remaining nonmagnetic fraction. Zircons were poured en masse onto double-sided sticky tape, while the other three minerals were hand-picked in order to avoid the other minerals occurring in those fractions. Mounts were imaged by SEM-CL at Boston College.

3.2. LA-ICP-MS Geochronology

All analyses were conducted with a CETAC LSX-213 G2+ 213 nm Nd:YAG laser ablation unit with a Helex two-volume ablation cell coupled to an Agilent 7900 quadrupole ICP-MS in the Material Characterization Laboratory of the Core Research Facility at the University of Massachusetts Lowell. Full instrumental parameters are given in the supporting information. All minerals were analyzed in blocks of about 10 unknowns

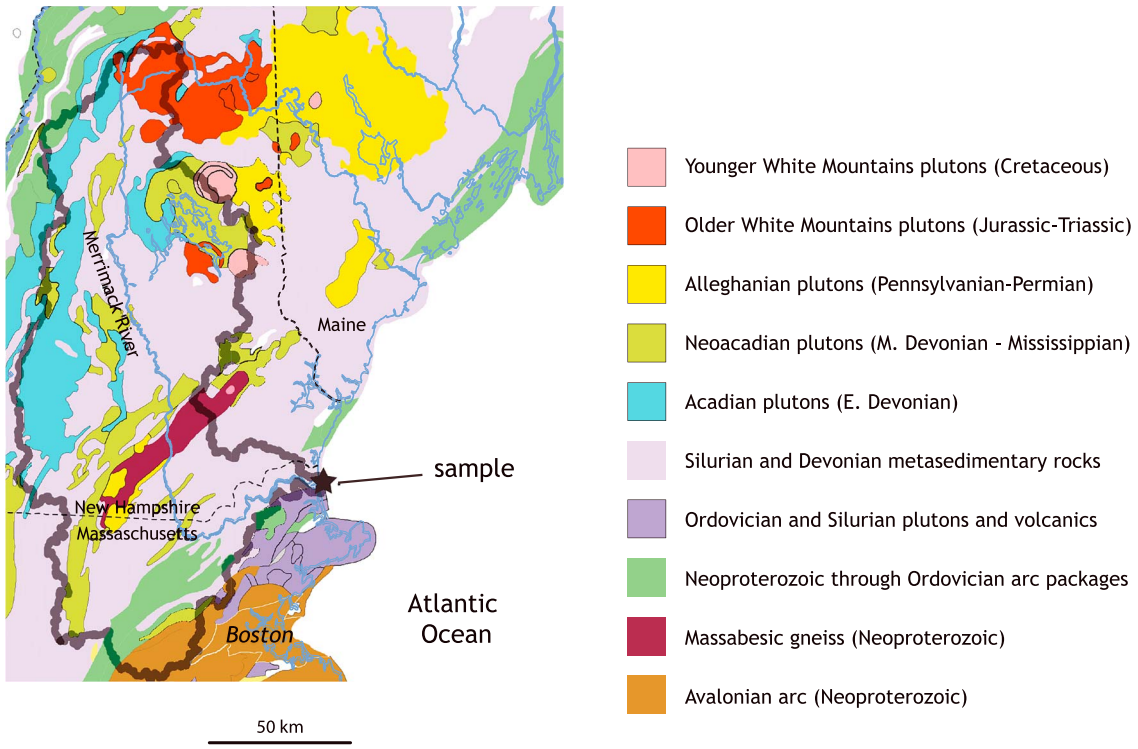

Figure 1. Major geologic units in drainage basin of the Merrimack River in New England, USA, modified from Bradley et al. (2015).

bracketed by analyses of a primary and secondary standard. Ablations generally targeted mineral rims, although several rutile core-rim pairs were analyzed. Analyses were approximately 45 s long, separated by 20 s for signal washout and gas blank measurement. All data were reduced with Iolite software (Paton et al., 2010). Quoted uncertainties include the internal error on the measurements of the unknowns propagated with the excess uncertainty derived from the primary standard during the session.

3.2.1. Zircon

Zircon analyses were conducted at a 7-Hz laser repetition rate with a 40-μm spot size. Plesovice (337.2 ± 0.1 Ma; Sláma et al., 2008; Horstwood et al., 2016) was used as a primary standard. FC-1 (1,099.0 ± 0.6 Ma; Paces & Miller, 1993) was used as a second standard and yielded a weighted mean $^{207}Pb/^{206}Pb$ age of 1,103 ± 5 Ma, within error of the accepted age. Concentrations for select trace elements were determined simultaneously with age data. NIST-610 was used as an external standard, and Si was used as an internal standard, with an assumed concentration of 15% by weight based on stoichiometry.

3.2.2. Monazite

Monazite analyses were conducted at a 7-Hz laser repetition rate with a 15-μm spot size. The 44069 monazite (424.9 ± 0.4 Ma; Aleinikoff et al., 2006) was used as a primary standard, and Trebilcock (272 ± 2 Ma; Tomascak et al., 1996) was used as a secondary standard, the latter yielding a weighted mean $^{207}Pb/^{235}U$ age of 274 ± 2 Ma, within error of the accepted age (the $^{207}Pb/^{235}U$ age is given because Trebilcock is reversely discordant due to excess ^{206}Pb from ^{230}Th). For simultaneous trace element analysis, P was used as an internal standard, with concentration set to 13% based on stoichiometry. The concentration of P in the NIST glasses is very low and near or below the detection limit when using the small spot size and laser energy required for monazite geochronology. Consequently, the Trebilcock standard was used as an external calibrant, using concentrations from McFarlane and McCulloch (2007).

3.2.3. Rutile

Rutile analyses were conducted at an 8-Hz laser repetition rate with a 50-μm spot size. Sugluk-4 (1,719 ± 14 Ma; Bracciali et al., 2013) was used as a primary standard. PCA-2S07 (1,865.0 ± 7.5 Ma; Bracciali et al., 2013) was used as a secondary standard and yielded a weighted mean age of 1,890 ± 11 Ma, slightly older than the best estimate age reported by Bracciali et al. (2013), likely reflecting

the contribution of the common Pb that has been noted in this standard. Trace elements were measured simultaneously using NIST-610 as an external calibrant and Ti as an internal standard (set to 58.7%, assuming TiO_2 = 98%).

Zr concentration in rutile is temperature dependent (Zack, Moraes, & Kronz, 2004). The calibration of Tomkins et al. (2007) for the Zr-in-rutile thermometer was used, and this incorporates a pressure dependence. The influence of pressure is quite small; for example, the difference in calculated temperature between 5 and 10 kbar of pressure is only ~20 °C. Temperatures calculated here are based on a model pressure of 8 kbar, which is reasonable given the repeated high grade metamorphism experienced in New England (e.g., Robinson et al., 1998).

3.2.4. Titanite

Titanite analyses were conducted at a 8-Hz laser repetition rate with a 40-μm sspot size. MKED-1 (1,521.02 ± 0.55 Ma; Spandler et al., 2016) was used as a primary standard. BLR-1 (1,047.1 ± 0.4 Ma; Aleinikoff et al., 2007) was used as a secondary standard and yielded a $^{207}Pb/^{206}Pb$ age of 1,046 ± 10 Ma. Trace elements were measured simultaneously using NIST-610 as an external calibrant and Si as an internal standard (set to 14.3% based on stoichiometry).

3.2.5. Common Pb Corrections on U-Pb Ages

The influence of common Pb on U-Pb analyses cannot be directly corrected due to the traces of Hg in the He carrier gas, contributing an isobaric overlap from ^{204}Hg on ^{204}Pb, which is present in small quantities. For Phanerozoic U-Pb dates, such as the vast majority of the dates presented here, common Pb can be the primary source of minor discordance, which is easily recognizable on Tera-Wasserburg diagrams. A "^{207}Pb correction," using a model common Pb $^{207}Pb/^{206}Pb$ ratio, can be used to correct for common Pb (Williams, 1998). For zircon and monazite, only a few analyses plotted above concordia (in Tera-Wasserburg space) and ^{207}Pb corrections did not shift the $^{206}Pb/^{238}U$ ages, so these corrections were not applied. In contrast, about a third of the rutiles analyzed here showed variable degrees of discordance that are most likely due to the presence of small amounts of common Pb coupled with the low levels of radiogenic Pb due to low U and (relatively) young age, and all of the titanites analyzed showed discordance attributable to common Pb. A ^{207}Pb correction was applied to these discordant rutile and titanite analyses, using a $^{207}Pb/^{206}Pb$ of 0.85 ± 0.05. This is a reasonable range based on published common Pb for the region (Ayuso & Bevier, 1991; Eby, 1985).

4. Results

U-Pb and trace element results are shown in Figures 2–9 and tabulated in the supporting information.

4.1. Zircons

Zircon age results are shown in Figure 2. Eighty-six percent of the 106 analyses yielded $^{207}Pb/^{206}Pb$ ages within error of $^{206}Pb/^{238}U$ ages and are hence considered concordant. Paleozoic ages are abundant, with a continuum of ages between 360 and 500 Ma, centered on a main peak at 406 Ma. Minor peaks are present at 123 and 193 Ma, and a few Neoproterozoic and Mesoproterozoic ages are also present. The age spectrum is quite similar to the detrital zircon spectrum for the same locality reported by Bradley et al. (2015; see supporting information).

Some key characteristics of the trace element compositions of the zircons are shown in Figure 3. A subset of the ~406-Ma zircons show markedly different trace element ratios compared to the rest of the data set, including unusually low Th/U and Ce/Yb and high U/Yb and Gd/Yb. Another distinct trace element feature is the elevated Nb/Yb ratios observed in several of the ~193-Ma zircons.

4.2. Monazite

Monazite age results are shown in Figure 4. Sixty-one of 66 analyses yielded $^{207}Pb/^{206}Pb$ ages within error of $^{206}Pb/^{238}U$ ages and are hence considered concordant. Due to monazite's strong affinity for Th, incorporation of ^{230}Th during crystallization can lead to the formation of excess ^{206}Pb and result in reverse discordance in young monazite (Parrish, 1990; Schärer, 1984), but this was not observed. While greatest precision was obtained on $^{208}Pb/^{232}Th$ ages, the lack of isotope dilution-thermal ionization mass spectrometer data for the Th-Pb system in the monazite standards means that concordance with U-Pb dates, while assumed, has not necessarily been verified. Therefore, $^{206}Pb/^{238}U$ ages are considered to be the most reliable. All

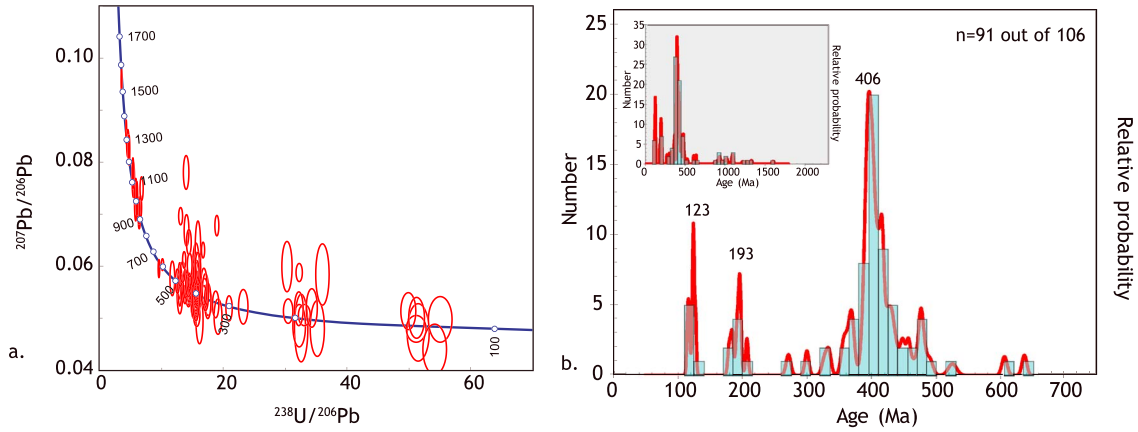

Figure 2. U-Pb geochronology results for detrital zircons. (a) Tera-Wasserberg diagram showing all results. Error ellipses here and in subsequent figures include internal error on individual measurements propagated with excess scatter on the primary standard, shown at the 2σ level. (b) Probability density curve and histogram for concordant zircon analyses (i.e., analyses where ^{207}Pb/^{206}Pb age is within uncertainty of the ^{206}Pb/^{238}U age). Inset shows full data set while the expanded panel zooms in on the Phanerozoic portion of the age spectrum. *N* provides the number of analyses plotted in the probability density plot out of the total number of analyses, here and in succeeding figures.

monazite ages are Phanerozoic, and nearly all are Paleozoic. A sharp and dominant age peak is present at ~389 Ma, a minor peak is present at ~347 Ma, and a continuum of ages are present from 250 to 298 Ma, with a broad peak around 277 Ma.

Key trace element characteristics of the monazites are shown in Figure 5. Compared to the other populations, the ~389-Ma population is characterized by considerably greater enrichment of middle rare earth elements over heavy rare earth elements, defined by the chondrite normalized Gd/Lu (Figure 5a) and a

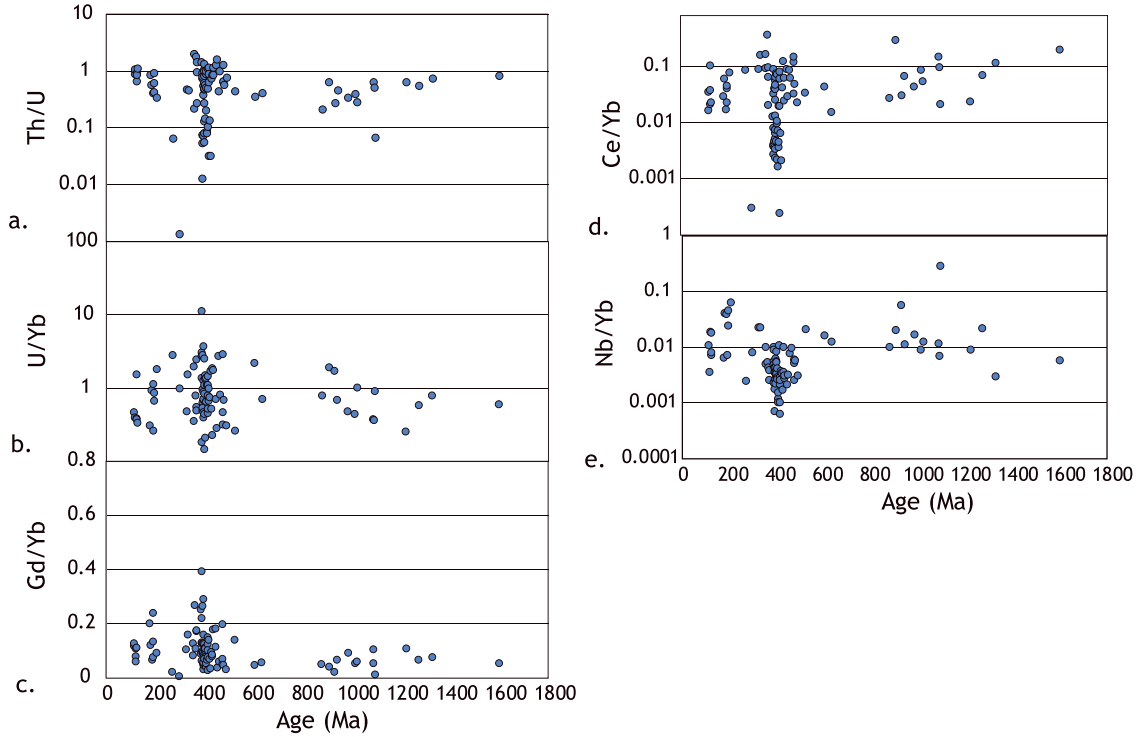

Figure 3. Trace element ratios from zircons, measured simultaneously with U-Pb age. All ratios share an excursion around 400 Ma, characterized by a subset of zircons in this age with either anomalously high or low ratios compared to the rest of the data set. (a–c) The low Th/U, high U/Yb, and high Gd/Yb of these 400 Ma grains is interpreted to reflect crystallization in equilibrium with igneous monazite from a highly peraluminous melt formed during crustal thickening. (d) The low Ce/Yb of these grains, driven by Ce depletion, is consistent with this explanation. (e) An important feature of the Nb/Yb data set is the presence of high values for many of the Early Jurassic zircons, consistent with the derivation from the A-type granites of the older White Mountains province.

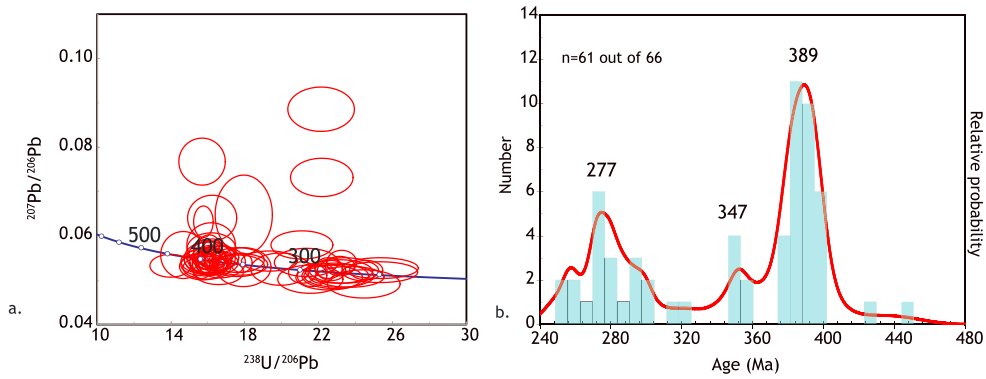

Figure 4. Monazite U-Pb age results with (a) Tera-Wasserberg diagram and (b) histogram and probability density curve of $^{206}Pb/^{238}U$ ages.

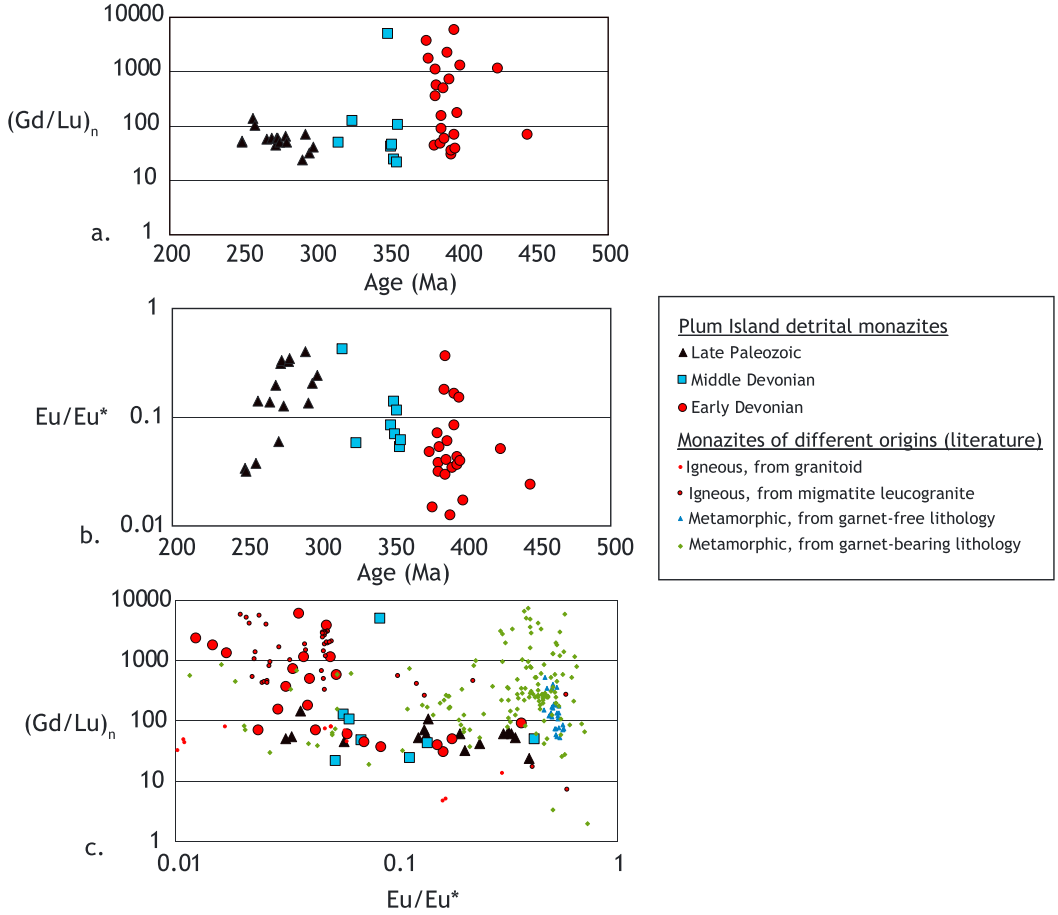

Figure 5. Trace element ratios from monazites, measured simultaneously with U-Pb age. Monazites are grouped and color coded by age. Many of the Early Devonian monazites have a (a) dramatically higher chondrite normalized Gd/Lu and (b) a more negative Eu anomaly than the other two age groups. The inverse relationship between these parameters is shown in (c), along with published results for monazites from various lithologies (Bea, 1996; Rubatto et al., 2006; Buick et al., 2010; Mottram et al., 2014; Štípská et al., 2015; Holder et al., 2015; Itano et al., 2018). Monazites crystallized from melt (in both granitoids and migmatites) consistently have a low Eu/Eu*, similar to the Early Devonian monazites observed in this study.

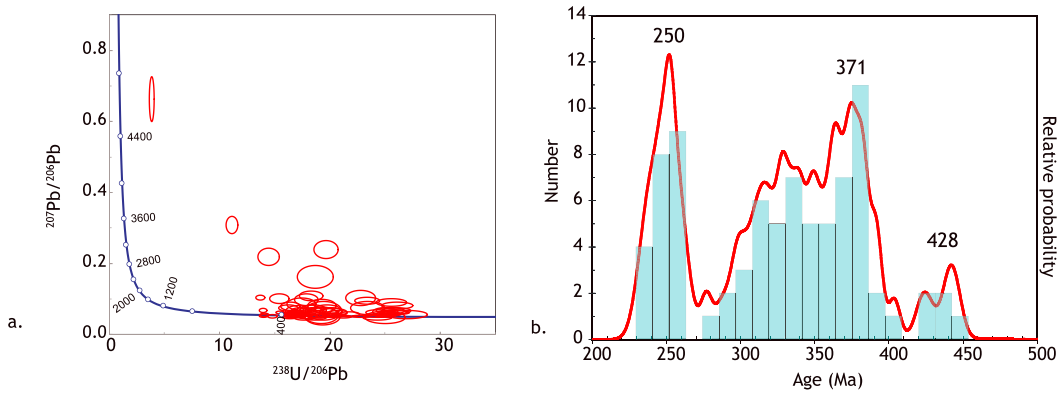

Figure 6. Rutile U-Pb age results with (a) Tera-Wasserberg diagram and (b) histogram and probability density curve of common Pb corrected ^{206}Pb/^{238}U ages.

considerably deeper negative Eu anomaly (defined as Eu_n/Eu_n^*, where $Eu_n^* = (Sm_n \times Gd_n)^{0.5}$ and "n" indicates chondrite normalized concentration).

4.3. Rutile

Rutile age results are shown in Figure 6. A significant fraction of analyzed rutiles show discordance attributable to common Pb, an effect magnified by low U and hence low radiogenic Pb present in some of the grains. Concordant ages and common Pb-corrected discordant ages are entirely Phanerozoic. A few Ordovician and Silurian ages are present, and a large number of grains display a continuum of ages between ~380 and 280 Ma. A narrow and sharp age peak is also present at 250 Ma.

Rutile has the lowest closure temperature of the phases studied here, and rutile grains formed under lower crustal conditions (i.e., with histories of prolonged, slow cooling) have been reported as having gradients of decreasing U-Pb age from crystal center to rim (e.g., Kooijman et al., 2010; Smye & Stockli, 2014). Consequently, dates were obtained for both the center and rim of several grains, but none showed a difference in age beyond uncertainty.

Trace element characteristics of the rutiles are shown in Figure 7. Most rutiles have relatively low Cr concentrations and moderate to high Nb concentrations although a small subset of grains has low Nb and high Cr (Figure 7a). Several of the low Nb rutiles have similar ages, around 350–360 Ma (Figure 7b). Zr-in-rutile thermometry, using the calibration of Tomkins et al. (2007) and a model pressure of 8 kbar, yields amphibolite-facies temperatures, with slightly higher values seen in the oldest rutiles.

4.4. Titanite

Titanite age results are shown in Figure 8. All analyzed titanite shows variable degrees of discordance attributable to common Pb. A large subset of analyses appears to trace out a linear array in Tera-Wasserburg space (Figure 8a) with a lower intercept age of 373±5 Ma, and the individual common Pb corrected ^{206}Pb/^{238}U ages are characterized by a dominant ~374-Ma peak. A continuum of ages between 400 and 480 Ma is also observed, along with two Permian ages.

Trace element characteristics are shown in Figure 9. Most grains have a molar Al/Fe ratio between 1 and 3. The Th/U shows a weak negative correlation with Al/Fe. Grains with anomalously high Al/Fe and low Th/U are primarily between 350 and 400 Ma (Figure 9c).

5. Discussion

The Phanerozoic U-Pb age results for the four detrital minerals are directly compared in Figure 10. Zircon ages record major events in the Ordovician through Early Devonian followed by a paucity of ages in the remainder of the Paleozoic. In contrast, monazite and rutile both show major age populations in the Middle and Late Devonian and the Permian. The majority of titanite ages overlap with a minor zircon age population. Furthermore, differences are present in the trace element compositions of different mineral age populations, most notably for zircon and monazite. Below, the ability of trace element compositions

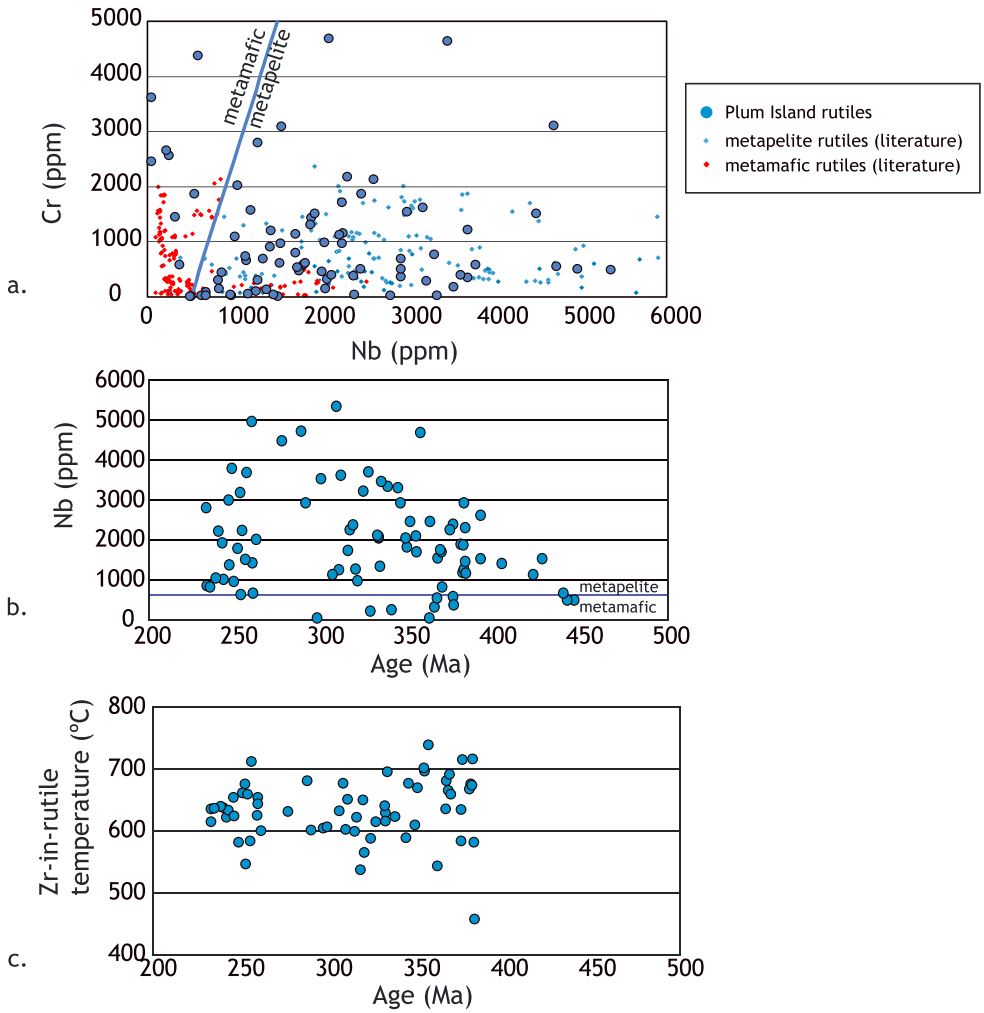

Figure 7. Rutile trace element characteristics and zirconium thermometry. (a) Nb-Cr covariation has been used frequently as a way of discriminating between rutile derived from metapelites and metamafic rocks (Meinhold et al., 2008; Triebold et al., 2007, 2012; Zack, von Eynatten, & Kronz, 2004). The divider here is taken from Triebold et al. (2007) and indicates that the vast majority of rutile were derived from metapelites. Published rutile data from Zack et al. (2002) and Zack, Moraes, & Kronz (2004a) and Luvizotto et al. (2009) are shown for comparison; metamafic rutile from the Catalina schist in California has unusually high Nb and low Cr, but all other rutile plots in the correct zones. (b) Rutile that was derived from the metamafic rocks is characterized by Nb less than 600 ppm. When Nb is plotted against age, metamafic rutiles are consistently older than 300 Ma. (c) Zr-in-rutile thermometry versus age, using the calibration of Tomkins et al. (2007). Temperature is calculated based on a model pressure of 8 kbar, but the thermometer's sensitivity to pressure is quite low. All rutile crystallized at amphibolite facies conditions, and the oldest grains skew toward slightly hotter temperatures.

to identify source lithologies is evaluated, and the combined age and geochemical information are used to link the detrital minerals to their source rocks. Finally, differences in provenance interpretation that would arise from analyzing only zircon or from not analyzing trace elements are discussed.

5.1. Source Rock Lithology From Detrital Mineral Trace Element Compositions

Trace element compositions of detrital accessory minerals may provide a diagnostic indicator for their source lithology and possibly its tectonic setting, and this possibility has been of particular interest with regards to zircon. The Th/U ratio has often been invoked as a discriminant between igneous and metamorphic zircon (Rubatto, 2002; Schaltegger et al., 1999), and a wider palette of elements has more recently been considered (Barth et al., 2013; Belousova et al., 2002; Cavosie et al., 2006; Grimes et al., 2009; Grimes et al., 2015; McKay et al., 2018; McKenzie et al., 2018; Nardi et al., 2013). In particular, Grimes et al. (2015) noted that ratios involving U, Nb, Sc, Yb, Gd, and Ce seemed to provide an effective means for

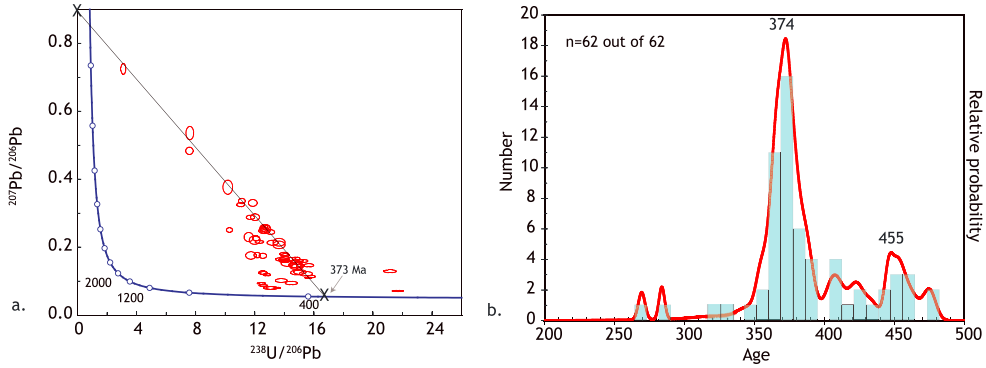

Figure 8. Titanite U-Pb age results with (a) Tera-Wasserberg diagram and (b) histogram and probability density curve of common Pb corrected $^{206}Pb/^{238}U$ ages. All grains have discordance attributable to common Pb content, and a significant fraction fall along a linear array between a common $^{207}Pb/^{206}Pb$ composition of 0.85 and a lower concordia intercept of 373 Ma.

distinguishing zircons formed from mantle-dominated settings (i.e., mid ocean ridges and ocean islands) from continental arc settings.

Several of these ratios are shown in Figure 3. The most striking feature of the data seen across multiple trace element ratios is the presence of anomalously high or low values in a subset of the ~400-Ma zircons. This includes the presence of low Th/U, Ce/Yb, and Nb/Yb and high U/Yb and Gd/Yb. In a conventional detrital zircon study where only ages and Th and U concentrations are obtained, these low Th/U zircons might be interpreted as being metamorphic in origin, but there is an alternate explanation that is supported by other ratios. Low Th/U ratios in zircon have been observed in some peraluminous granitoids (Gaschnig et al., 2010; McKay et al., 2018) and are most likely attributable to the formation in equilibrium with igneous monazite, which has a very strong affinity for Th (Bea, 1996; Breiter, 2016; Kirkland et al., 2015; Miles et al., 2013; Yakymchuk et al., 2018). Monazite also has a very strong affinity for light rare earth elements (Bea, 1996) and thus might also explain the low Ce/Yb seen in these zircons, which is driven almost entirely by low Ce concentrations (although Ce abundance in zircon can also be governed by melt oxygen fugacity; Trail et al., 2012). Derivation of these zircons from peraluminous granitoids, formed presumably by crustal melting in thickened crust (e.g., Gaschnig et al., 2011), is also consistent with the higher Gd/Yb and U/Yb, which have been interpreted as indicators of greater crustal thickness during magma generation and greater levels of crustal melting, respectively (Barth et al., 2013; Grimes et al., 2015).

Another important trace element characteristic is the high Nb/Yb seen in several of the Early Jurassic zircons. High field strength elements such as niobium are often enriched in A-type granites (Eby, 1992; Pearce et al., 1984), and Nb enrichment in zircons from such granites has been documented (Grimes et al., 2015; Nardi et al., 2013). Therefore, these zircons likely record an episode of A-type magmatism in the Merrimack drainage in the Early Jurassic.

The trace element composition of monazite may also provide clues to the type of lithology from which detrital grains originated. Itano et al. (2016, 2018) examined the rare earth element systematics and Th/U ratios of monazites from a variety of metamorphic and igneous rock types in order to develop the criteria for identifying source rock lithologies for detrital monazites. Itano et al. (2018) considered a significantly negative Eu anomaly (Eu/Eu* < 0.1) and only modest enrichment of light rare earth elements over middle rare earth elements ($Ce_n/Gd_n < 3$) to be diagnostic of igneous monazite derived from granitic rocks. They interpreted strong fractionation of the middle rare earth elements over the heavy rare earth elements ($Gd_n/Lu_n > 500$) as often diagnostic of metamorphic monazite derived from garnet-bearing rocks (i.e., garnet-bearing amphibolite and eclogite facies), although igneous monazites from garnet-bearing pegmatites and leucogranites associated with migmatites were also found to have similarly high fractionation.

Detrital monazites studied here are divisible into Devonian, Carboniferous, and Permian age groupings with differences in trace element geochemistry. The Devonian grains extend to distinctly high Gd/Lu values and have especially deep negative Eu anomalies on average compared to the other two groups. Metamorphic monazites rarely have Eu/Eu* values less than 0.1 (Itano et al., 2018, and references therein), so it seems

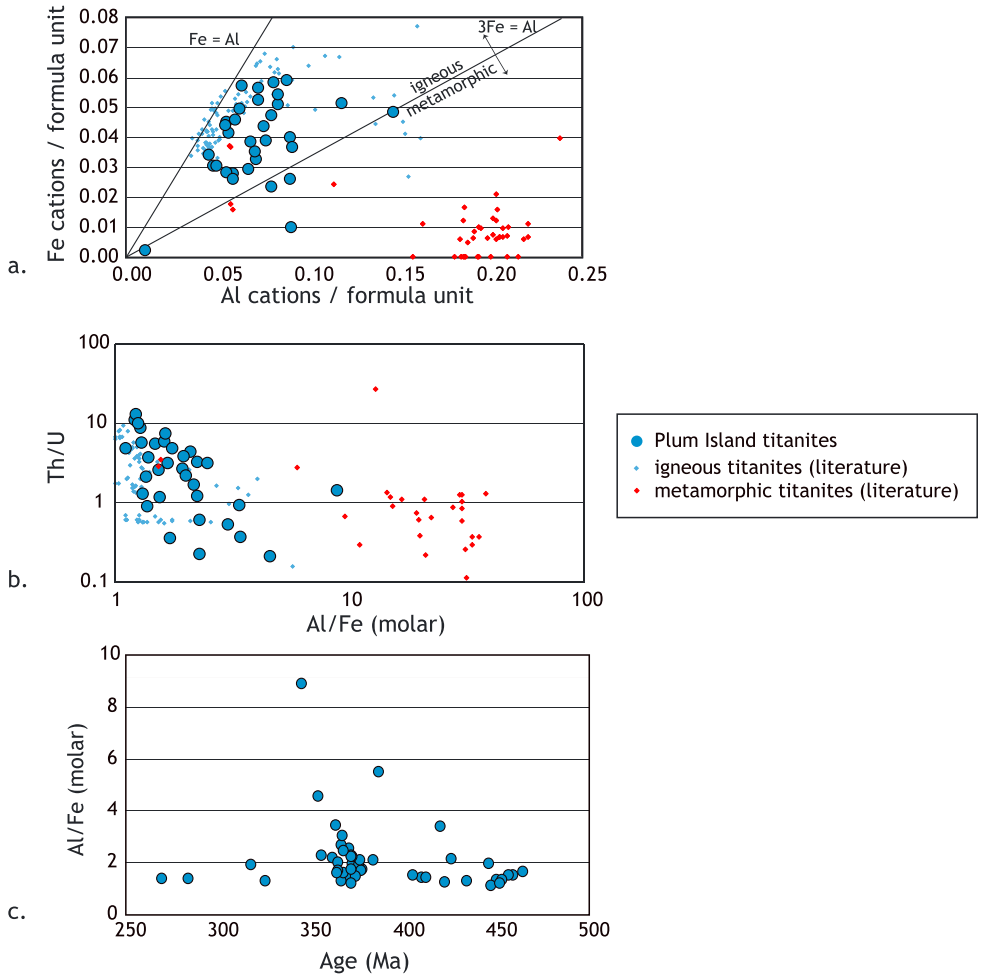

Figure 9. Titanite trace element characteristics. (a) The relative content of Fe and Al can be used as a discriminant between igneous and metamorphic titanite, with Al/Fe > 3 being considered diagnostic of metamorphic titanite (Aleinikoff et al., 2002). Only a few such grains were observed here. Small red and blue points in (a) and (b) are igneous and metamorphic titanites, respectively, from literature sources (Aleinikoff et al., 2002; Gao et al., 2012; Pan et al., 2018; Rasmussen et al., 2013; Spandler et al., 2016). (b) Grains with high Al/Fe also have low Th/U, which is also considered to be an attribute of metamorphic titanite (Aleinikoff et al., 2002; Gao et al., 2012). (c) Titanite grains with the highest Al/Fe and of probable metamorphic origin are found between 400 and 350 Ma.

likely that many of the Devonian monazites formed as igneous phases in granitoids or migmatites. The high Gd/Lu seen in many of these same monazite grains may reflect equilibrium with igneous garnet, as both phases can occur in strongly peraluminous granites (and such rocks are present in this part of New England; see below), although this might also indicate origin in migmatites. Conversely, the considerably shallower Eu anomaly seen in the Permian monazites is suggestive of origin in metamorphic rocks, and the relatively low Gd/Lu indicates that these monazites did not form in equilibrium with garnet and are hence from garnet-free amphibolite or granulite facies rocks (Itano et al., 2018). The Carboniferous monazites show trace element characteristics that are intermediate between the Permian and Devonian monazites and may come from a mix of igneous and metamorphic source rocks.

Rutile Cr and Nb covariation can be used as a source rock discriminant; rutile crystallized in metapelites tends to have higher Nb and lower Cr than rutile formed in metamafic rocks (Meinhold et al., 2008; Triebold et al., 2007, 2012; Zack, von Eynatten, & Kronz, 2004). The majority of the rutile grains studied here have Nb and Cr concentrations consistent with derivation from metapelites. Of the minority of grains with metamafic trace element chemistry, several have similar ages around 350 to 360 Ma. Zr-in-rutile temperatures indicate that formation occurred during amphibolite facies metamorphism.

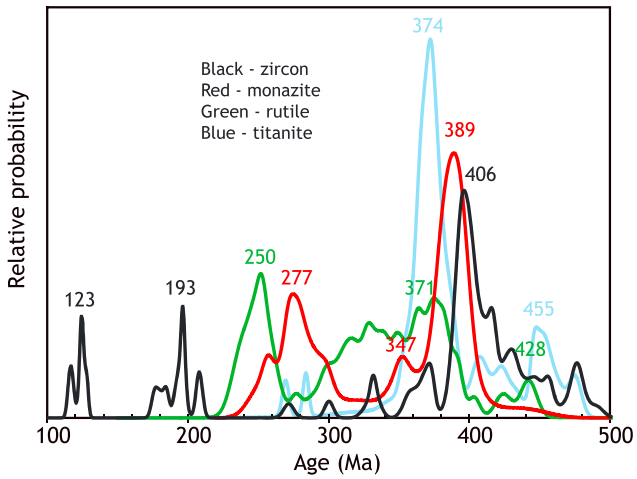

Figure 10. Probability density plot combining Phanerozoic age results for all four minerals from the Plum Island sand sample (note that some Precambrian zircons were observed and are shown in Figure 2 but not included here). Black = zircon, red = monazite, green = rutile, and blue = titanite. Monazite and rutile fill in gaps in the zircon record, especially in the late Paleozoic. Titanite age peaks correspond to minor zircon populations.

For titanite, the Al/Fe ratio has been used as a discriminant between igneous and metamorphic origin. Aleinikoff et al. (2002) noted that the metamorphic grains tend to have molar Al/Fe greater than 3. A Th/U less than 1 has also been used as an indicator of metamorphic origin (Aleinikoff et al., 2002; Schmitz et al., 2018), and Figure 9b shows an inverse correlation between these two parameters. Only a few titanite grains analyzed here show chemistry characteristic of metamorphic origin, and these tend to have ages between 350 and 400 Ma (Figure 9c).

5.2. Sediment Sources From Geochronology and Trace Element Geochemistry of Detrital Minerals

The zircon results provide baseline information on the igneous history of the region. A limited number of Proterozoic zircons were observed in the Plum Island sands, but these have no known igneous source in the Merrimack River drainage basin. It is conceivable that these zircons were derived from Pleistocene glacial deposits with sources outside of the drainage basin. However, in their study of detrital zircons in several major New England Rivers, Bradley et al. (2015) noted that the river sand zircon ages faithfully record the geologic history of their drainage basins and contain very little exotic glacial input. Consequently, the Precambrian Plum Island zircons are likely derived from some of the extensive Early Paleozoic metasedimentary sequences found throughout the drainage basin (Dorais et al., 2012; Wintsch et al., 2007).

The next significant geologic event recorded by the detrital minerals is Ordovician and Silurian magmatism, marked by a limited number of zircon and titanite ages. These grains were probably sourced from the Nashoba terrane, as no other rocks with appropriate ages are present within Merrimack drainage basin (Acaster & Bickford, 1999). Given that titanite is most common in metaluminous igneous rocks (Frost et al., 2001), which in turn are especially characteristic of island arcs and continental arcs with normal crustal thickness, the source rocks for the Ordovician and Silurian titanites are probably such arc rocks. The similarly aged zircons have trace element signatures that are also compatible with formation in arc rocks.

Major Devonian tectonomagmatic activity is recorded by all four detrital minerals. The largest zircon age population is centered at ~406 Ma, and many of these zircons show trace element characteristics consistent with formation in peraluminous granites formed by melting in thickened crust, possibly associated with terrane accretion/collision (i.e., the Acadian orogeny). These zircons were likely derived from the New Hampshire Plutonic Suite, which is exposed throughout southern and central New Hampshire and contains many plutons with appropriate compositions (Dorais, 2003; Dorais & Paige, 2000; Dorais & Tubrett, 2012). Several of these plutons contain garnet, and such plutons may have yielded many of the Devonian monazites (i.e., those that are characterized by both low Eu/Eu* and high Gd/Lu), although some portion of that monazite age population also was likely derived from Early Paleozoic migmatites and metasedimentary rocks that were experiencing metamorphism at the same time. The detrital rutile grains with a continuum of ages beginning at ~375 Ma and extending into the Carboniferous probably originated from the same Early Paleozoic metasedimentary rocks and record the same metamorphism as those monazites but reflect slow cooling and the lower closure temperature of the U-Pb system in rutile. This closure temperature is comparable to the K-Ar system in amphibole, and amphibole K-Ar ages in metasedimentary rocks of western New Hampshire and adjacent Massachusetts range from 407 to 280 Ma (Spear & Harrison, 1989), largely overlapping with the spread of Devonian to Carboniferous rutile ages. The Zr-in-rutile temperatures are consistent with the estimated peak temperatures for these metasedimentary rocks (Spear, 2002). The abundant ~385-Ma detrital titanite grains may have been derived from different, more metaluminous units of the New Hampshire Plutonic Suite than those that supplied the monazites, although they might have also been obtained from appropriately aged plutons in Massachusetts in the Lowell area (Walsh et al., 2013). The small number of younger monazite grains around ~350 Ma may record the Neoacadian orogeny (Robinson et al., 1998), and domains of appropriate age have been observed in monazites in migmatitic gneisses in southwest New Hampshire (Pyle et al., 2005), along with other localities in central Massachusetts and Connecticut

(Massey et al., 2017), further outside the drainage basin of the Merrimack River. The thermal imprint of this event may have also aided in producing the wide spread of Late Devonian and Carboniferous rutile ages.

Permian monazite ages record major Alleghanian metamorphism at ~277 Ma. These monazites were likely derived from the extensive Early Paleozoic metasedimentary rocks in southern New Hampshire and adjacent Massachusetts, as monazite of this age has been reported in those rocks (Eusden & Barreiro, 1988) and metamorphism this age has also been reported in the Neoproterozoic Massabesic gneiss in southern New Hampshire (Dorais et al., 2012). A sharply defined rutile age peak follows the monazite by approximately 15 Ma. Extensive Ar-Ar cooling data are available for the Massabesic gneiss and surrounding younger metasedimentary rocks (Dorais et al., 2012), and these may help pinpoint a likely source of these rutile grains. While both units experienced the Alleghanian thermal peak, the Massabesic cooled more slowly and would have passed through the rutile U-Pb closure temperature around the time of the detrital rutile age peak. The Massabesic gneiss is therefore a strong candidate for being the source of the Permo-Triassic rutile population. It is noteworthy that the shapes of the rutile age peaks (asymmetric with a long younging tail in the Devonian-Carboniferous but sharp in the Permian) are consistent with the broader thermal history of southeastern New England determined from U-Pb and Ar-Ar studies (e.g., Wintsch et al., 1992). Also noteworthy is the fact that this orogenic event was largely amagmatic in the Merrimack drainage basin and therefore left no sign in the detrital zircon record.

Detrital zircons record two magmatic events in the Mesozoic at 195 and 120 Ma. These ages are entirely consistent with the timings of magmatism in the older and younger White Mountains magmatic provinces (Eby et al., 1992), especially in light of new U-Pb geochronology showing that the duration of magmatism was comparably brief (Kinney et al., 2018). The Pemigewasset River, one of the two principal upper tributaries of the Merrimack River, originates in the White Mountain batholith of New Hampshire, which is the central feature of the older White Mountains magmatic province and likely the source of the 195-Ma zircons. The Ossippee pluton, one of the major elements of the younger White Mountains magmatic province (Roden-Tice et al., 2009), is located in the drainage basin of the Winnipesaukee River, the other principal tributary of the Merrimack, and is the likely source of the Cretaceous detrital zircons.

5.3. Benefits of Looking Beyond Detrital Zircon Ages in Provenance Research

A key point of this contribution is that zircon ages by themselves can provide an incomplete portrait of sediment sources and the geologic history of the source region. If the Plum Island sand had been collected from a river in a remote region for which little geologic knowledge existed and been subjected to a conventional detrital zircon study, one might conclude based on Figure 2 that the region in question contained limited exposures of Proterozoic basement and had experienced intense magmatism starting in the Ordovician and peaking in the Early Devonian. This was followed by quiescence interrupted only by further magmatism in the Early Jurassic and again in the Early Cretaceous. No information on the tectonic setting of these magmatic pulses or source lithology type can really be presumed from the ages alone, and there would be no sign of any Permian tectonomagmatic activity.

Expansion of the detrital mineral analytical toolkit to incorporate a limited palette of zircon trace element ratios measured simultaneously with U-Pb provides some constraints on the lithology type and tectonic setting of many of these zircons, indicating that the Early Devonian magmatic episode saw a significant amount of crustal melting in thickened crust, leading to the formation of peraluminous granites and suggestive of terrane accretion or continental collision (Figure 11). The Nb enrichment seen in the Early Jurassic zircons suggests an A-type granite origin, indicative of an intraplate and/or hot spot related setting.

Additional layers of information are provided by the ages and trace element characteristics of the other minerals (Figure 11). Ordovician-Silurian titanite grains (coupled with more “normal” trace element ratios for coeval zircons) record a more metaluminous period of magmatism more typical of an arc-type environment prior to the Early Devonian event. The Middle Devonian monazite population, containing a mix of magmatic and metamorphic grains, records continuing high grade metamorphism and associated crustal melting and the age offset and smeared nature of the U-Pb results for the Devonian rutile grains suggest a prolonged thermal disturbance and slow cooling in the region's metasedimentary package. This was followed by renewed high-grade metamorphism in the Permian, an event that is completely missed in the detrital zircon record.

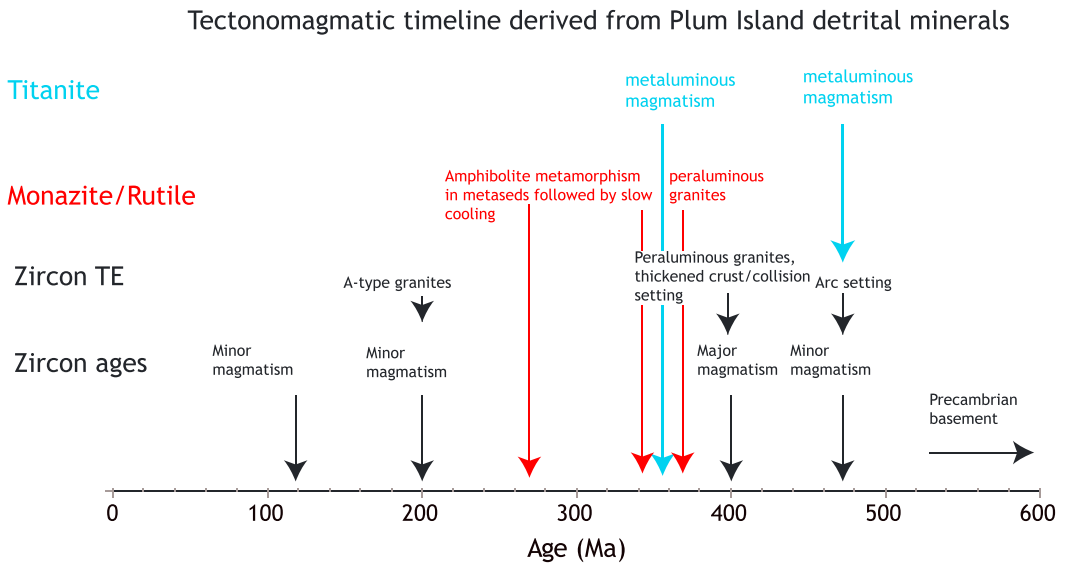

Figure 11. Schematic timeline depicting the layers of additional information provided by adding trace element analysis and U-Pb dating of other minerals to the baseline provided by the zircon ages. The trace elements in zircon suggest that the minor Ordovician age population formed in a typical arc setting, whereas the major Devonian population was derived from peraluminous granites formed in thickened crust probably associated with a terrane collision. Zircon trace elements also indicate that some of the Jurassic grains were derived from A-type granites. The oldest monazite population is probably igneous and records continued peraluminous magmatism, whereas the younger monazite and rutile populations record amphibolite grade metamorphism of metasedimentary rocks followed by slow cooling. The titanite ages line up with minor zircon age populations and are supportive of metaluminous magmatism at those times.

6. Conclusion

U-Pb age and trace element data presented here for different detrital minerals from the mouth of the Merrimack River (New England) demonstrate the great advantages to be gained in sedimentary and tectonic research when detrital mineral studies are expanded beyond just zircon dating. Monazite and rutile ages can provide a record of metamorphism in the sediment source region that may be completely absent from the detrital zircon record. Measurement of trace element ratios in detrital zircon and comparison of detrital zircon age spectra with those of detrital titanite provide important clues for determining the tectonic setting and/or bulk lithology of igneous rocks in the sediment source region, and trace elements also provide the means of providing information on the type of rocks that monazite and rutile were derived from, along with the temperature at which rutile grew. All of this information can be obtained using a single instrument package (i.e., quadrupole ICP-MS and laser) with moderate capital costs.

Acknowledgments
This work would not have been possible without the geochronology standards generously provided by several researchers, notably John Aleinikoff, Chris Fisher, George Gehrels, Matt Horstwood, and Carl Spandler. I also thank Joe Kopera for sharing his knowledge of New England geology, Dwight Bradley for sharing his map files, Keita Itano for sharing his monazite trace element database, and Earl Ada for helping install and maintain the ICP-MS. Data associated with this paper are found in the supporting information. This paper was improved by reviews from Glenn Sharman and two anonymous reviewers.

References

Acaster, M., & Bickford, M. E. (1999). Geochronology and geochemistry of Putnam-Nashoba terrane metavolcanic and plutonic rocks, eastern Massachusetts: Constraints on the early Paleozoic evolution of eastern North America. *Geological Society of America Bulletin*, *111*(2), 240–253. https://doi.org/10.1130/0016-7606(1999)111<0240:GAGOPN>2.3.CO;2

Aleinikoff, J. N., Schenck, W. S., Plank, M. O., Srogi, L., Fanning, C. M., Kamo, S. L., & Bosbyshell, H. (2006). Deciphering igneous and metamorphic events in high-grade rocks of the Wilmington Complex, Delaware: Morphology, cathodoluminescence and backscattered electron zoning, and SHRIMP U-Pb geochronology of zircon and monazite. *Geological Society of America Bulletin*, *118*(1–2), 39–64. https://doi.org/10.1130/b25659.1

Aleinikoff, J. N., Wintsch, R. P., Fanning, C. M., & Dorais, M. J. (2002). U–Pb geochronology of zircon and polygenetic titanite from the Glastonbury Complex, Connecticut, USA: An integrated SEM, EMPA, TIMS, and SHRIMP study. *Chemical Geology*, *188*(1–2), 125–147. https://doi.org/10.1016/S0009-2541(02)00076-1

Aleinikoff, J. N., Wintsch, R. P., Tollo, R. P., Unruh, D. M., Fanning, C. M., & Schmitz, M. D. (2007). Ages and origins of rocks of the Killingworth dome, south-central Connecticut: Implications for the tectonic evolution of southern New England. *American Journal of Science*, *307*(1), 63–118. https://doi.org/10.2475/01.2007.04

Ayuso, R. A., & Bevier, M. L. (1991). Regional differences in Pb isotopic compositions of feldspars in plutonic rocks of the northern Appalachian Mountains, U.S.A., and Canada: A geochemical method of terrane correlation. *Tectonics*, *10*(1), 191–212. https://doi.org/10.1029/90TC02132

Barth, A. P., Wooden, J. L., Jacobson, C. E., & Economos, R. C. (2013). Detrital zircon as a proxy for tracking the magmatic arc system: The California arc example. *Geology*, *41*(2), 223–226. https://doi.org/10.1130/G33619.1

Bea, F. (1996). Residence of REE, Y, Th and U in granites and crustal protoliths: Implications for the chemistry of crustal melts. *Journal of Petrology*, *37*, 552–521.

Belousova, E., Griffin, W., O'Reilly, S. Y., & Fisher, N. (2002). Igneous zircon: Trace element composition as an indicator of source rock type. *Contributions to Mineralogy and Petrology*, *143*(5), 602–622. https://doi.org/10.1007/s00410-002-0364-7

Bracciali, L., Parrish, R. R., Horstwood, M. S. A., Condon, D. J., & Najman, Y. (2013). UPb LA-(MC)-ICP-MS dating of rutile: New reference materials and applications to sedimentary provenance. *Chemical Geology*, *347*(0), 82–101. https://doi.org/10.1016/j.chemgeo.2013.03.013

Bradley, D., & Tucker, R. (2002). Emsian synorogenic paleogeography of the Maine Appalachians. *The Journal of Geology*, *110*(4), 483–492. https://doi.org/10.1086/340634

Bradley, D. C., O'Sullivan, P., & Bradley, L. M. (2015). Detrital zircons from modern sands in New England and the timing of Neoproterozoic to Mesozoic magmatism. *American Journal of Science*, *315*(5), 460–485. https://doi.org/10.2475/05.2015.03

Breiter, K. (2016). Monazite and zircon as major carriers of Th, U, and Y in peraluminous granites: Examples from the Bohemian Massif. *Mineralogy and Petrology*, *110*(6), 767–785. https://doi.org/10.1007/s00710-016-0448-0

Buick, I. S., Clark, C., Rubatto, D., Hermann, J., Pandit, M., & Hand, M. (2010). Constraints on the Proterozoic evolution of the Aravalli–Delhi orogenic belt (NW India) from monazite geochronology and mineral trace element geochemistry. *Lithos*, *120*(3-4), 511–528. https://doi.org/10.1016/j.lithos.2010.09.011

Cavosie, A. J., Valley, J. W., & Wilde, S. A. (2006). Correlated microanalysis of zircon: Trace element, $\delta^{18}O$, and U–Th–Pb isotopic constraints on the igneous origin of complex >3900 Ma detrital grains. *Geochimica et Cosmochimica Acta*, *70*(22), 5601–5616. https://doi.org/10.1016/j.gca.2006.08.011

Clift, P. D., Shimizu, N., Layne, G. D., & Blusztajn, J. (2001). Tracing patterns of erosion and drainage in the Paleogene Himalaya through ion probe Pb isotope analysis of detrital K-feldspars in the Indus Molasse, India. *Earth and Planetary Science Letters*, *188*(3–4), 475–491. https://doi.org/10.1016/S0012-821X(01)00346-6

Copeland, P., Bertrand, G., France-Lanord, C., & Sundell, K. (2015). $^{40}Ar/^{39}Ar$ ages of muscovites from modern Himalayan rivers: Himalayan evolution and the relative contribution of tectonics and climate. *Geosphere*, *11*(6), 1837–1859. https://doi.org/10.1130/ges01154.1

Dorais, M. J. (2003). The petrogenesis and emplacement of the New Hampshire plutonic suite. *American Journal of Science*, *303*(5), 447–487 . https://doi.org/10.2475/ajs.303.5.447

Dorais, M. J., & Paige, M. L. (2000). Regional geochemical and isotopic variations of northern New England plutons: Implications for magma sources and for Grenville and Avalon basement-terrane boundaries. *GSA Bulletin*, *112*(6), 900–914. https://doi.org/10.1130/0016-7606(2000)112<900:RGAIVO>2.0.CO;2

Dorais, M. J., & Tubrett, M. (2012). Detecting peritectic garnet in the peraluminous Cardigan Pluton, New Hampshire. *Journal of Petrology*, *53*(2), 299–324. https://doi.org/10.1093/petrology/egr063

Dorais, M. J., Wintsch, R. P., Kunk, M. J., Aleinikoff, J., Burton, W., Underdown, C., & Kerwin, C. M. (2012). *P-T-t* conditions, Nd and Pb isotopic compositions and detrital zircon geochronology of the Massabesic Gneiss Complex, New Hampshire: Isotopic and metamorphic evidence for the identification of Gander basement, central New England. *American Journal of Science*, *312*(10), 1049–1097. https://doi.org/10.2475/10.2012.01

Eby, G. N. (1985). Sr and Pb isotopes, U and Th chemistry of the alkaline Monteregian and White Mountain igneous provinces, eastern North America. *Geochimica et Cosmochimica Acta*, *49*(5), 1143–1153. https://doi.org/10.1016/0016-7037(85)90005-5

Eby, G. N. (1992). Chemical subdivision of the A-type granitoids: Petrogenetic and tectonic implications. *Geology*, *20*(7), 641–644. https://doi.org/10.1130/0091-7613(1992)020<0641:CSOTAT>2.3.CO;2

Eby, G. N., Krueger, H. W., & Creasy, J. W. (1992). Geology, geochronology, and geochemistry of the White Mountain batholith, New Hampshire. *Eastern North American Mesozoic Magmatism*, *268*, 379–398. https://doi.org/10.1130/SPE268-p379

Eriksson, K. A., Campbell, I. H., Palin, J. M., & Allen, C. M. (2003). Predominance of Grenvillian magmatism recorded in detrital zircons from modern Appalachian rivers. *Journal of Geology*, *111*(6), 707–717. https://doi.org/10.1086/378338

Eriksson, K. A., Campbell, I. H., Palin, J. M., Allen, C. M., & Bock, B. (2004). Evidence for multiple recycling in Neoproterozoic through Pennsylvanian sedimentary rocks of the central Appalachian Basin. *Journal of Geology*, *112*(3), 261–276. https://doi.org/10.1086/382758

Eusden, J. D. Jr., & Barreiro, B. (1988). The timing of peak high-grade metamorphism in central-eastern New England. *Maritime Sediments and Atlantic Geology*, *24*(3), 241–255.

Frost, B. R., Chamberlain, K. R., & Schumacher, J. C. (2001). Sphene (titanite): Phase relations and role as a geochronometer. *Chemical Geology*, *172*(1–2), 131–148. https://doi.org/10.1016/S0009-2541(00)00240-0

Gao, X.-Y., Zheng, Y.-F., Chen, Y.-X., & Guo, J. (2012). Geochemical and U–Pb age constraints on the occurrence of polygenetic titanites in UHP metagranite in the Dabie orogen. *Lithos*, *136-139*, 93–108. https://doi.org/10.1016/j.lithos.2011.03.020

Gaschnig, R. M., Vervoort, J. D., Lewis, R. S., & McClelland, W. C. (2010). Migrating magmatism in the northern US Cordillera: In situ U–Pb geochronology of the Idaho batholith. *Contributions to Mineralogy and Petrology*, *159*(6), 863–883. https://doi.org/10.1007/s00410-009-0459-5

Gaschnig, R. M., Vervoort, J. D., Lewis, R. S., & Tikoff, B. (2011). Isotopic evolution of the Idaho batholith and Challis intrusive province, northern US cordillera. *Journal of Petrology*, *52*(12), 2397–2429. https://doi.org/10.1093/petrology/egr050

Gehrels, G. (2015). Detrital zircon U-Pb geochronology applied to tectonics. *Annual Review of Earth and Planetary Sciences*, *42*(1), 127–149.

Gray, M. B., & Zeitler, P. K. (1997). Comparison of clastic wedge provenance in the Appalachian foreland using U/Pb ages of detrital zircons. *Tectonics*, *16*(1), 151–160. https://doi.org/10.1029/96TC02911

Grimes, C. B., John, B. E., Cheadle, M. J., Mazdab, F. K., Wooden, J. L., Swapp, S., & Schwartz, J. J. (2009). On the occurrence, trace element geochemistry, and crystallization history of zircon from in situ ocean lithosphere. *Contributions to Mineralogy and Petrology*, *158*(6), 757–783. https://doi.org/10.1007/s00410-009-0409-2

Grimes, C. B., Wooden, J. L., Cheadle, M. J., & John, B. E. (2015). "Fingerprinting" tectono-magmatic provenance using trace elements in igneous zircon. *Contributions to Mineralogy and Petrology*, *170*(5–6), 1–26.

Hietpas, J., Samson, S., Moecher, D., & Schmitt, A. K. (2010). Recovering tectonic events from the sedimentary record: Detrital monazite plays in high fidelity. *Geology*, *38*(2), 167–170. https://doi.org/10.1130/G30265.1

Hodges, K. V., Ruhl, K. W., Wobus, C. W., & Pringle, M. S. (2005). $^{40}Ar/^{39}Ar$ thermochronology of detrital minerals. In P. W. Reiners & T. A. Ehlers (Eds.), *Low temperature thermochronology: Techniques, interpretation, and applications* (pp. 239–257). Chantilly, VA: Mineralogical Society of America

Holder, R. M., Hacker, B. R., Kylander-Clark, A. R. C., & Cottle, J. M. (2015). Monazite trace-element and isotopic signatures of (ultra)high-pressure metamorphism: Examples from the Western Gneiss Region, Norway. *Chemical Geology*, *409*, 99–111. https://doi.org/10.1016/j.chemgeo.2015.04.021

Horstwood, M. S. A., Košler, J., Gehrels, G., Jackson, S. E., McLean, N. M., Paton, C., et al. (2016). Community-derived standards for LA-ICP-MS U-(Th-)Pb geochronology—Uncertainty propagation, age interpretation and data reporting. *Geostandards and Geoanalytical Research*, *40*(3), 311–332. https://doi.org/10.1111/j.1751-908X.2016.00379.x

Iizuka, T., Campbell, I. H., Allen, C. M., Gill, J. B., Maruyama, S., & Makoka, F. (2013). Evolution of the African continental crust as recorded by U-Pb, Lu-Hf and O isotopes in detrital zircons from modern rivers. *Geochimica et Cosmochimica Acta*, *107*, 96–120. https://doi.org/10.1016/j.gca.2012.12.028

Itano, K., Iizuka, T., Chang, Q., Kimura, J.-I., & Maruyama, S. (2016). U–Pb chronology and geochemistry of detrital monazites from major African rivers: Constraints on the timing and nature of the Pan-African Orogeny. *Precambrian Research*, *282*, 139–156. https://doi.org/10.1016/j.precamres.2016.07.008

Itano, K., Iizuka, T., & Hoshino, M. (2018). REE-Th-U and Nd isotope systematics of monazites in magnetite- and ilmenite-series granitic rocks of the Japan arc: Implications for its use as a tracer of magma evolution and detrital provenance. *Chemical Geology*, *484*, 69–80. https://doi.org/10.1016/j.chemgeo.2017.11.033

Kinney, S. T., J. B. Setera, P. E. Olsen, S. A. MacLennan, J. A. VanTongeren, B. Schoene, et al. (2018), Causal implications of new geochronological constraints on Mesozoic post-rift magmatism in New England, *Goldschmidt Abstracts*.

Kirkland, C. L., Smithies, R. H., Taylor, R. J. M., Evans, N., & McDonald, B. (2015). Zircon Th/U ratios in magmatic environs. *Lithos*, *212*, 397–414.

Kooijman, E., Mezger, K., & Berndt, J. (2010). Constraints on the U-Pb systematics of metamorphic rutile from in situ LA-ICP-MS analysis. *Earth and Planetary Science Letters*, *293*(3–4), 321–330. https://doi.org/10.1016/j.epsl.2010.02.047

LaMaskin, T. A. (2012). Detrital zircon facies of cordilleran terranes in western North America. *GSA Today*, *22*(3), 4–11.

Luvizotto, G. L., Zack, T., Triebold, S., & von Eynatten, H. (2009). Rutile occurrence and trace element behavior in medium-grade metasedimentary rocks: Example from the Erzgebirge, Germany. *Mineralogy and Petrology*, *97*(3-4), 233–249. https://doi.org/10.1007/s00710-009-0092-z

Lyons, J. B., W. A. Bothner, R. H. Moench, and J. B. Thompson, Jr. (1997), Bedrock geologic map of New Hampshire, USGS.

Massey, M. A., Moecher, D. P., Walker, T. B., O'Brien, T. M., & Rohrer, L. P. (2017). The role and extent of dextral transpression and lateral escape on the post-Acadian tectonic evolution of south-central New England. *American Journal of Science*, *317*(1), 34–94. https://doi.org/10.2475/01.2017.02

McFarlane, C. R. M., & McCulloch, M. T. (2007). Coupling of in-situ Sm–Nd systematics and U–Pb dating of monazite and allanite with applications to crustal evolution studies. *Chemical Geology*, *245*(1-2), 45–60. https://doi.org/10.1016/j.chemgeo.2007.07.020

McKay, M. P., Jackson, W. T., & Hessler, A. M. (2018). Tectonic stress regime recorded by zircon Th/U. *Gondwana Research*, *57*, 1–9. https://doi.org/10.1016/j.gr.2018.01.004

McKenzie, N. R., Smye, A. J., Hegde, V. S., & Stockli, D. F. (2018). Continental growth histories revealed by detrital zircon trace elements: A case study from India. *Geology*, *46*(3), 275–278. https://doi.org/10.1130/G39973.1

Meinhold, G., Anders, B., Kostopoulos, D., & Reischmann, T. (2008). Rutile chemistry and thermometry as provenance indicator: An example from Chios Island, Greece. *Sedimentary Geology*, *203*(1-2), 98–111. https://doi.org/10.1016/j.sedgeo.2007.11.004

Miles, A. J., Graham, C. M., Hawkesworth, C. J., Gillespie, M. R., Hinton, R. W., & Edinburgh Ion Microprobe Facility (EIMF) (2013). Evidence for distinct stages of magma history recorded by the compositions of accessory apatite and zircon. *Contributions to Mineralogy and Petrology*, *166*(1), 1–19. https://doi.org/10.1007/s00410-013-0862-9

Moecher, D., & Samson, S. (2006). Differential zircon fertility of source terranes and natural bias in the detrital zircon record: Implications for sedimentary provenance analysis. *Earth and Planetary Science Letters*, *247*(3–4), 252–266. https://doi.org/10.1016/j.epsl.2006.04.035

Morag, N., Avigad, D., Gerdes, A., Belousova, E., & Harlavan, Y. (2011). Detrital zircon Hf isotopic composition indicates long-distance transport of North Gondwana Cambrian-Ordovician sandstones. *Geology*, *39*(10), 955–958. https://doi.org/10.1130/G32184.1

Mottram, C. M., Warren, C. J., Regis, D., Roberts, N. M. W., Harris, N. B. W., Argles, T. W., & Parrish, R. R. (2014). Developing an inverted Barrovian sequence; Insights from monazite petrochronology. *Earth and Planetary Science Letters*, *403*, 418–431. https://doi.org/10.1016/j.epsl.2014.07.006

Naeser, C. W., Naeser, N. D., Newell, W. L., Southworth, S., Edwards, L. E., & Weems, R. E. (2016). Erosional and depositional history of the Atlantic passive margin as recorded in detrital zircon fission-track ages and lithic detritus in Atlantic coastal plain sediments. *American Journal of Science*, *316*(2), 110–168. https://doi.org/10.2475/02.2016.02

Nardi, L. V. S., Formoso, M. L. L., Muller, I. F., Fontana, E., Jarvis, K., & Lamarao, C. (2013). Zircon/rock partition coefficients of REEs, Y, Th, U, Nb, and Ta in granitic rocks: Uses for provenance and mineral exploration purposes. *Chemical Geology*, *335*, 1–7. https://doi.org/10.1016/j.chemgeo.2012.10.043

O'Sullivan, G. J., Chew, D. M., & Samson, S. D. (2016). Detecting magma-poor orogens in the detrital record. *Geology*, *44*(10), 871–874. https://doi.org/10.1130/G38245.1

Paces, J. B., & Miller, J. D. Jr. (1993). Precise U-Pb ages of Duluth Complex and related mafic intrusions, northeastern Minnesota: Geochronological insights to physical, petrogenetic, paleomagnetic, and tectonomagmatic processes associated with the 1.1 Ga Midcontinent Rift System. *Journal of Geophysical Research*, *98*(B8), 13,997–14,013. https://doi.org/10.1029/93JB01159

Painter, C. S., Carrapa, B., DeCelles, P. G., Gehrels, G. E., & Thomson, S. N. (2014). Exhumation of the North American Cordillera revealed by multi-dating of Upper Jurassic-Upper Cretaceous foreland basin deposits. *Geological Society of America Bulletin*, *126*(11–12), 1439–1464. https://doi.org/10.1130/b30999.1

Pan, L.-C., Hu, R.-Z., Bi, X.-W., Li, C., Wang, X.-S., & Zhu, J.-J. (2018). Titanite major and trace element compositions as petrogenetic and metallogenic indicators of Mo ore deposits: Examples from four granite plutons in the southern Yidun arc, SW China. *American Mineralogist*, *103*(9), 1417–1434. https://doi.org/10.2138/am-2018-6224

Parrish, R. R. (1990). U–Pb dating of monazite and its application to geological problems. *Canadian Journal of Earth Sciences*, *27*(11), 1431–1450. https://doi.org/10.1139/e90-152

Paton, C., Woodhead, J. D., Hellstrom, J. C., Hergt, J. M., Greig, A., & Maas, R. (2010). Improved laser ablation U-Pb zircon geochronology through robust downhole fractionation correction. *Geochemistry, Geophysics, Geosystems*, *11*, Q0AA06. https://doi.org/10.1029/2009GC002618

Pearce, J. A., Harris, N. B. W., & Tindle, A. G. (1984). Trace element discrimination diagrams for the tectonic interpretation of granitic rocks. *Journal of Petrology*, *25*(4), 956–983. https://doi.org/10.1093/petrology/25.4.956

Pyle, J. M., Spear, F. S., Cheney, J. T., & Layne, G. (2005). Monazite ages in the Chesham Pond Nappe, SW New Hampshire, U.S.A.: Implications for assembly of central New England thrust sheets. *American Mineralogist*, *90*(4), 592–606. https://doi.org/10.2138/am.2005.1341

Rasmussen, B., Fletcher, I. R., & Muhling, J. R. (2013). Dating deposition and low-grade metamorphism by in situ UPb geochronology of titanite in the Paleoproterozoic Timeball Hill Formation, southern Africa. *Chemical Geology*, *351*, 29–39. https://doi.org/10.1016/j.chemgeo.2013.04.015

Reiners, P. W. (2005). (U-Th)/(He-Pb) double dating of detrital zircons. *American Journal of Science*, *305*(4), 259–311. https://doi.org/10.2475/ajs.305.4.259

Robinson, P., Tucker, R. D., Bradley, D., Berry Iv, H. N., & Osberg, P. H. (1998). Paleozoic orogens in New England, USA. *GFF*, *120*(2), 119–148. https://doi.org/10.1080/11035899801202119

Roden-Tice, M. K., West, D. P. Jr., Potter, J. K., Raymond, S. M., & Winch, J. L. (2009). Presence of a long-term lithospheric thermal anomaly: Evidence from apatite fission-track analysis in northern New England. *Journal of Geology*, *117*(6), 627–641. https://doi.org/10.1086/605995

Rubatto, D. (2002). Zircon trace element geochemistry: Partitioning with garnet and the link between U-Pb ages and metamorphism. *Chemical Geology*, *184*(1–2), 123–138. https://doi.org/10.1016/S0009-2541(01)00355-2

Rubatto, D., Hermann, J., & Buick, I. S. (2006). Temperature and bulk composition control on the growth of monazite and zircon during low-pressure anatexis (Mount Stafford, Central Australia). *Journal of Petrology*, *47*(10), 1973–1996. https://doi.org/10.1093/petrology/egl033

Schaltegger, U., Fanning, C. M., Günther, D., Maurin, J. C., Schulmann, K., & Gebauer, D. (1999). Growth, annealing and recrystallization of zircon and preservation of monazite in high-grade metamorphism: Conventional and in-situ U-Pb isotope, cathodoluminescence and microchemical evidence. *Contributions to Mineralogy and Petrology*, *134*(2-3), 186–201. https://doi.org/10.1007/s004100050478

Schärer, U. (1984). The effect of initial ^{230}Th disequilibrium on young U-Pb ages: The Makalu case, Himalaya. *Earth and Planetary Science Letters*, *67*(2), 191–204. https://doi.org/10.1016/0012-821X(84)90114-6

Schmitz, M. D., Southwick, D. L., Bickford, M. E., Mueller, P. A., & Samson, S. D. (2018). Neoarchean and Paleoproterozoic events in the Minnesota River Valley subprovince, with implications for southern Superior craton evolution and correlation. *Precambrian Research*, *316*, 206–226. https://doi.org/10.1016/j.precamres.2018.08.010

Slagstad, T., & Kirkland, C. L. (2017). The use of detrital zircon data in terrane analysis: A nonunique answer to provenance and tectonostratigraphic position in the Scandinavian Caledonides. *Lithosphere*, *9*(6), 1002–1011. https://doi.org/10.1130/L663.1

Sláma, J., Košler, J., Condon, D. J., Crowley, J. L., Gerdes, A., Hanchar, J. M., et al. (2008). Plešovice zircon—A new natural reference material for U–Pb and Hf isotopic microanalysis. *Chemical Geology*, *249*(1–2), 1–35. https://doi.org/10.1016/j.chemgeo.2007.11.005

Smye, A. J., & Stockli, D. F. (2014). Rutile U–Pb age depth profiling: A continuous record of lithospheric thermal evolution. *Earth and Planetary Science Letters*, *408*, 171–182. https://doi.org/10.1016/j.epsl.2014.10.013

Spandler, C., Hammerli, J., Sha, P., Hilbert-Wolf, H., Hu, Y., Roberts, E., & Schmitz, M. (2016). MKED1: A new titanite standard for in situ analysis of Sm–Nd isotopes and U–Pb geochronology. *Chemical Geology*, *425*, 110–126. https://doi.org/10.1016/j.chemgeo.2016.01.002

Spear, F. S. (2002). Metamorphic, thermal, and tectonic evolution of central New England. *Journal of Petrology*, *43*(11), 2097–2120. https://doi.org/10.1093/petrology/43.11.2097

Spear, F. S., & Harrison, T. M. (1989). Geochronologic studies in central New England I: Evidence for pre-Acadian metamorphism in eastern Vermont. *Geology*, *17*(2), 181–184. https://doi.org/10.1130/0091-7613(1989)017<0181:GSICNE>2.3.CO;2

Stewart, E. D., Link, P. K., Fanning, C. M., Frost, C. D., & McCurry, M. (2010). Paleogeographic implications of non-North American sediment in the Mesoproterozoic upper Belt Supergroup and Lemhi Group, Idaho and Montana, USA. *Geology*, *38*(10), 927–930. https://doi.org/10.1130/G31194.1

Štípská, P., Hacker, B. R., Racek, M., Holder, R., Kylander-Clark, A. R. C., Schulmann, K., & Hasalová, P. (2015). Monazite dating of prograde and retrograde *P–T–d* paths in the Barrovian terrane of the Thaya window, Bohemian Massif. *Journal of Petrology*, *56*(5), 1007–1035. https://doi.org/10.1093/petrology/egv026

Thomas, W. A., Becker, T. P., Samson, S. D., & Hamilton, M. A. (2004). Detrital zircon evidence of a recycled orogenic foreland provenance for Alleghanian clastic wedge sandstones. *Journal of Geology*, *112*(1), 23–37. https://doi.org/10.1086/379690

Thompson, M. D., Barr, S. M., & Grunow, A. M. (2012). Avalonian perspectives on Neoproterozoic paleogeography: Evidence from Sm-Nd isotope geochemistry and detrital zircon geochronology in SE New England, USA. *Geological Society of America Bulletin*, *124*(3–4), 517–531. https://doi.org/10.1130/B30529.1

Tomascak, P. B., Krogstad, E. J., & Walker, R. J. (1996). U-Pb monazite geochronology of granitic rocks from Maine: Implications for late Paleozoic tectonics in the northern Appalachians. *The Journal of Geology*, *104*(2), 185–195. https://doi.org/10.1086/629813

Tomkins, H. S., Powell, R., & Ellis, D. J. (2007). The pressure dependence of the zirconium-in-rutile thermometer. *Journal of Metamorphic Geology*, *25*(6), 703–713. https://doi.org/10.1111/j.1525-1314.2007.00724.x

Trail, D., Bruce Watson, E., & Tailby, N. D. (2012). Ce and Eu anomalies in zircon as proxies for the oxidation state of magmas. *Geochimica et Cosmochimica Acta*, *97*, 70–87. https://doi.org/10.1016/j.gca.2012.08.032

Triebold, S., von Eynatten, H., Luvizotto, G. L., & Zack, T. (2007). Deducing source rock lithology from detrital rutile geochemistry: An example from the Erzgebirge, Germany. *Chemical Geology*, *244*(3-4), 421–436. https://doi.org/10.1016/j.chemgeo.2007.06.033

Triebold, S., von Eynatten, H., & Zack, T. (2012). A recipe for the use of rutile in sedimentary provenance analysis. *Sedimentary Geology*, *282*, 268–275. https://doi.org/10.1016/j.sedgeo.2012.09.008

Tyrrell, S., Haughton, P. D. W., Daly, J. S., Kokfelt, T. F., & Gagnevin, D. (2006). The use of the common Pb isotope composition of detrital K-feldspar grains as a provenance tool and its application to Upper Carboniferous paleodrainage, northern England. *Journal of Sedimentary Research*, *76*(2), 324–345. https://doi.org/10.2110/jsr.2006.023

Walsh, G. J., Aleinikoff, J. N., Wintsch, R. P., & Ayuso, R. A. (2013). Integrated bedrock mapping and geochronology in the terranes of southeastern New England. *Geological Society of America, Abstracts with Programs*, *45*(1).

Williams, I. S. (1998). U-Th-Pb geochronology by ion microprobe. *Reviews in Economic Geology*, *7*, 1–35.

Wintsch, R. P., Aleinikoff, J. N., Walsh, G. J., Bothner, W. A., Hussey, A. M. II, & Fanning, C. M. (2007). SHRIMP U-Pb evidence for a Late Silurian age of metasedimentary rocks in the Merrimack and Putnam-Nashoba terranes, eastern New England. *American Journal of Science*, *307*(1), 119–167. https://doi.org/10.2475/01.2007.05

Wintsch, R. P., Sutter, J. F., Kunk, M. J., Aleinikoff, J. N., & Dorais, M. J. (1992). Contrasting *P-T-t* paths: Thermochronologic evidence for a late Paleozoic final assembly of the Avalon composite terrane in the New England Appalachians. *Tectonics*, *11*(3), 672–689. https://doi.org/10.1029/91TC02904

Yakymchuk, C., Kirkland, C. L., & Clark, C. (2018). Th/U ratios in metamorphic zircon. *Journal of Metamorphic Geology*, *36*(6), 715–737. https://doi.org/10.1111/jmg.12307

Zack, T., Kronz, A., Foley, S. F., & Rivers, T. (2002). Trace element abundances in rutiles from eclogites and associated garnet mica schists. *Chemical Geology*, *184*(1-2), 97–122. https://doi.org/10.1016/S0009-2541(01)00357-6

Zack, T., Moraes, R., & Kronz, A. (2004). Temperature dependence of Zr in rutile: Empirical calibration of a rutile thermometer. *Contributions to Mineralogy and Petrology*, *148*(4), 471–488. https://doi.org/10.1007/s00410-004-0617-8

Zack, T., Stockli, D. F., Luvizotto, G. L., Barth, M. G., Belousova, E., Wolfe, M. R., & Hinton, R. W. (2011). In situ U-Pb rutile dating by LA-ICP-MS: ^{208}Pb correction and prospects for geological applications. *Contributions to Mineralogy and Petrology*, *162*(3), 515–530. https://doi.org/10.1007/s00410-011-0609-4

Zack, T., von Eynatten, H., & Kronz, A. (2004). Rutile geochemistry and its potential use in quantitative provenance studies. *Sedimentary Geology*, *171*(1–4), 37–58. https://doi.org/10.1016/j.sedgeo.2004.05.009